ARTICLES

Computer Simulation Study of the Density and Temperature Dependence of Fundamental and Overtone Vibrational Dephasing in Nitrogen: Interplay between Different Mechanisms of Dephasing

N. Gayathri[†] and B. Bagchi*[,†,‡]

Solid State and Structural Chemistry Unit, Indian Institute of Science, Bangalore 560 012, India, and Department of Chemistry, University of Wisconsin, Madison, Wisconsin 53706

Received: May 11, 1999; In Final Form: September 13, 1999

Vibrational phase relaxation of the fundamental and the overtones of the N−N stretch of nitrogen in pure nitrogen has been studied by extensive molecular dynamics simulations. The thermodynamic state points simulated include states near the melting point, the boiling point, and the critical point, a normal liquid away from the transition, and also supercritical nitrogen. The simulations provide the following results. (1) The well-known result of Clouter and Kiefte (*J. Chem. Phys.* **1977**, *66*, 1736) on the pronounced insensitivity of vibrational phase relaxation of the fundamental to the change in thermodynamic conditions from the triple point (TP) to beyond the boiling point (BP) is found to originate from a competition between density relaxation and resonant energy transfer terms. The latter becomes increasingly important as the melting point is approached. (2) It is found that the experimentally observed *sharp rise* in the relaxation rate near the gas−liquid critical point (CP) can be attributed at least partly to the sharp rise in the contribution of vibration−rotation coupling. (3) The sharp rise in the vibration−rotation coupling in turn leads, *in an unusual way*, to a substantial subquadratic quantum number dependence of the overtone dephasing rate near the critical point and in supercritical fluids. The quantum number dependence, however, is found to be quadratic in the condensed phase. (4) The quantum number dependence of overtone dephasing is found to be critically dependent on the separation of time scales between the relaxations of the frequency modulation time correlation function and the normal coordinate time correlation function. The two decays must overlap to observe a significant subquadratic quantum number dependence. The latter is found to occur in the supercritical fluid state. (5) In the absence of a clear separation of time scales between the frequency modulation and the normal coordinate time correlation functions and because of the pronounced Gaussian decay of the latter, the Kubo−Oxtoby method of correlating the motionally narrowing limit with a homogeneous line shape becomes ambiguous. (6) An interesting *crossover behavior* across the liquid−gas phase transition region is observed in the density−temperature dependencies of the overtone dephasing rate. This crossover is most pronounced for higher overtones. (7) Although the simulation results reproduce the experimental data semiquantitatively (within 40% in most cases) and get the trends correct, quantitative agreement has not been achieved. We attribute this to the large number of terms (correlations and cross-correlations) which contribute to dephasing. In addition, the change of pair intermolecular potential with the thermodynamic state may itself play an increasingly important role, particularly in supercritical fluids.

1. Introduction

Vibrational phase relaxation (VR) of a molecular bond vibration arises from a delicate balance between several interactions that exist within the liquid. Therefore, it is a powerful tool to probe the interactions of a chemical bond with its surrounding medium.[1] The time scales of these molecular interactions cover a wide range from the ultrafast (collisional interactions) to the almost static (attractive force interactions).

It is widely believed that vibrational dephasing occurs mainly due to three processes arising out of molecular interactions, namely, the phase relaxation or pure vibrational dephasing due to elastic processes, the resonant transfer between different molecules, and the vibrational energy relaxation due to inelastic transitions.[1−3] Pure dephasing involves the continuous, stochastic fluctuations of the energy levels of a molecule interacting with its surroundings. It is usually the dominant dephasing mechanism and is also often much faster than the other above-mentioned dephasing processes. Resonant transfer effects on the line width (observed using isotopic dilution studies[4]) is found to be about 10−20% and is often much less; population relaxation studies[5] have shown that it is slower than dephasing by factors ranging from 4 to 10^{12}. Therefore, while it is generally sufficient to consider the effect of pure dephasing on line shapes, the time scales of the above processes could be comparable and

* Corresponding author. E-mail: bbagchi@sscu.iisc.ernet.in.
† Indian Institute of Science.
‡ University of Wisconsin.

10.1021/jp9915533 CCC: $18.00
Published on Web 11/06/1999

their interplay could result in strong cross-correlations between them in some cases.[3] Also, another mechanism which can contribute substantially, albeit in not very dense systems, is the vibrational−rotational coupling.[6,7]

Traditionally, vibrational phase relaxation has been studied by two types of experiment, both based on Raman scattering techniques.[1,3] The simpler approach is the study of the isotropic Raman line shape. The other method involves a coherent excitation of the vibration with a laser pulse and monitoring the decay of the phase coherence after a delay time by anti-Stokes Raman scattering measurements at the phase-matched angle. The latter method is particularly useful in cases where the Raman line is broadened by isotope splittings. Neither experiment allows a separation of the pure dephasing contribution from the resonant transfer and population relaxation contributions. Moreover, with such techniques, only fundamentals and lower overtones of the vibrational modes can be studied.

Systematic studies of vibrational dephasing using such techniques have been carried out in a large number of molecular liquids to observe dephasing and its dependence on temperature, pressure, and concentration.[3,6,8,9] Methods used involve temperature or pressure variations, isotopic dilution, or comparative line width measurements for several different Raman-active transitions in a given molecule.[2,9] For example, Clouter and Kiefte[9] had investigated the Raman line width of nitrogen and oxygen along the coexistence curve from the triple point, through the boiling point, to the critical point. The line widths (directly proportional to the rate of vibrational phase relaxation) were found to increase rapidly as the critical point was approached, in both systems, probably due to the rapidly decreasing density in that temperature range.[2] As the temperature was lowered from the normal boiling point to the triple point, the line width of O_2 increased by a factor of 2, whereas that for N_2 remained approximately constant.

The isotropic Raman line widths of liquid nitrogen and oxygen have also been measured by Clements and Stoicheffi[10] and by Scotto[11] and were found to be significantly smaller than the corresponding gas phase line widths. The increased broadening in the gas phase is due to the larger vibration−rotation coupling contribution because of nearly free rotation of the molecules in the low-density and high-temperature gaseous state than in the liquid phase.[12] We have recently addressed the enhanced role of vibration−rotation coupling in the dephasing of nitrogen near the critical point.[13]

While the vibration−rotation contribution to the line width is not expected to be large in the liquid phase and may be negligible in some cases, particularly highly dense systems such as CH_3I,[14] it may still be important in the case of *liquid* N_2, as shown by Brueck.[12] The work of Brueck indicated the importance of vibration−rotation coupling for nitrogen even at denser liquid state densities.

Experimental investigations in a wide range of systems have clearly indicated a strong dependence of the dephasing rate on the density and the temperature of the system. A few cases related to N_2 and CH_3I studies are mentioned below. LeDuff[15] studied the Raman band shape of N_2 dissolved in inert solvents (SF_6, CCl_4, $CHCl_3$, and SO_2). The observed full widths at half-height ranged from 1 to 1.3 cm^{-1}, indicating motional narrowing by a factor of more than 2 compared to the gas, but much less than in liquid nitrogen. Hesp et al.[16] measured the dephasing rate of N_2 as a function of concentration in liquid mixtures of N_2 and Ar, using both picosecond and Raman line shape techniques. The two methods were in agreement and showed a reduction in the dephasing time, τ_v, for the fundamental from 174 ps for pure N_2 to 70 ps in dilute Ar solutions. This reduction can be qualitatively understood in a hydrodynamic model since the viscosity of Ar is twice that of N_2.

Wright et al.[17] and others[18] have carried out temperature-dependent studies *at constant pressure* of the line width of ν_3 of C−I stretch. They observed a narrowing of the line width as the temperature was raised in the liquid phase. Since a constant-pressure experiment involves simultaneous changes in temperature and density, it was unclear which was the primary cause of the narrowing. Pressure-dependent studies by Jonas and coworkers[19] provided the answer. They found that the line width remained approximately constant for temperature changes at constant density, and it increased with increasing density at constant temperature. The constant-pressure results are thus due entirely to the expansion of the liquid on heating.

Since dephasing is expected to be correlated with the time correlation function of the force on the vibrational coordinate, most theoretical studies have predicted strong dependence of the dephasing rate on the viscosity of the liquid. The binary collision model[20] predicts a line width proportional to $\eta\rho^{-1}T$, the hydrodynamic theory[1] ηT, and Lynden-Bell's theory[24] $\eta\rho T^{-1}$. However, while these theories could explain different cases of study, *they have considered only the atom−atom interactions to dephasing and have not included the resonance-energy transfer and vibrational−rotational terms that could be significant in many cases*.[14,21,22] An earlier simulation study of the dephasing of the A_1 modes of model liquid methyl cyanide[23] at several state points clearly revealed the inadequacies of the above theories. The same study was also able to show how the physical state of the liquid critically affects the amplitude and dynamics of the fluctuations in the forces that act along the normal vibrational modes, and how these factors in turn have a bearing on the dephasing of the modes. A generic theory that could explain the dephasing behavior over the broad density and temperature range that exists between the liquid−solid and the liquid−gas coexistence has yet to be developed. Moreover, recent nonlinear optical techniques, such as fifth- and seventh-order responses from the vibrational mode (wherein a laser pulse excites a coherent superposition of vibrational modes and a second probe pulse sent after a delay time τ measures the decay of relaxation processes which occur in the time scale of τ), using which higher quantum levels are accessible,[25−28] have revealed many interesting new results, such as the subquadratic observations of the dephasing rate (directly proportional to the line width) as a function of quantum number n of the overtone[6,8] (as against the theoretically predicted quadratic dependence on n) in some systems. For example, in systems like $CDCl_3$ and CD_3I, the ratio of the dephasing rates between the overtone and the fundamentals of the C−D stretching mode is 2.1 and 2.4, respectively,[8] as against the theoretically expected value of 4 in both systems. Overtone transition studies that have been attempted earlier[29,30] have reported similar subquadratic quantum number dependence, although these observations involved a considerable amount of uncertainty because of low signal-to-noise factors of the bandwidth measurements.

Note that none of the above-mentioned theories can satisfactorily explain the observed subquadratic quantum number dependence of the dephasing rate. That the situation is somewhat complex can be understood from the following analysis. The average dephasing time $\langle\tau_{vn}\rangle$ for the nth overtone is given by[1]

$$\langle\tau_{vn}\rangle = \int_0^\infty \mathrm{d}t\, \langle Q(t)\, Q(0)\rangle_{n0} \qquad (1)$$

where $Q(t)$ is the time-dependent normal coordinate whose

dephasing is being studied and $\langle Q(t)\ Q(0)\rangle_{n0}$ is the relevant time correlation function for the *n*th overtone. The Fourier transform of this function is the observable in isotropic Raman experiments. The quadratic dependence of the dephasing rate $\langle\tau_{vn}\rangle^{-1}$ on the quantum number *n* arises when $\langle Q(t)\ Q(0)\rangle_{n0}$ decays exponentially as The above form is well-known and is the one

$$\langle Q(t)\ Q(0)\rangle_{n0} = \exp(-n^2 t/\tau) \qquad (2)$$

usually assumed in the Kubo−Oxtoby theory. In addition, all the theoretical studies (except the one reported in ref 14) assume a clear separation of time scales between the decay of $\langle Q(0)\ Q(t)\rangle$ and the frequency modulation time correlation function. For many systems, the latter assumption also breaks down, particularly for higher overtones.

In a dense liquid, the decay of the vibrational correlation function is *not* single exponential. It is expected to be biphasic with a Gaussian decay at short times followed by an exponential decay at longer times.[6,7,14] Now if the decay of $\langle Q(t)\ Q(0)\rangle_{n0}$ is fully Gaussian as in the following form:

$$\langle Q(t)\ Q(0)\rangle_{n0} = \exp(-n^2 t^2/\tau^2) \qquad (3)$$

then the dependence of $\langle\tau_{vn}\rangle^{-1}$ on *n* is *linear*. Thus, the quantum number dependence will critically depend on the relative magnitudes of the two components of the biphasic decay. It was earlier believed that in dense liquids the Gaussian component was negligible. For example, in Oxtoby's work, the force−force correlation function (which is required to determine $\langle Q(t)\ Q(0)\rangle_{n0}$) related to friction is assumed to be delta-correlated.[1] Microscopic calculation of the frequency-dependent friction (based on the recently developed mode-coupling theory (MCT))[31,32] and computer simulations[13,33,34] have clearly demonstrated that the force−force correlation function (or dynamic friction) has a rich structure and is certainly not delta-correlated. The time-dependent friction on the normal coordinate is found to have the universal nonexponential characteristics in both systems—a distinct inertial Gaussian part followed by a slower almost-exponential part. The main point here is that although $\langle Q(t)\ Q(0)\rangle_{n0}$ may show a largely quadratic *n* dependence (in the exponential), the experimental observables, such as $\langle\tau_{vn}\rangle$ or the width of the Raman line shape function, can show subquadratic *n* dependence. The microscopic calculations show that this can indeed happen.

In this article we present a detailed investigation on the temperature and density dependence of both fundamental and overtone dephasing of nitrogen. This can be considered as an extension of our earlier work where we studied dephasing only near the boiling point.[33] Simulations have now been carried out to determine the dephasing line widths in liquid N_2 at various state points ranging from the triple point to the critical point and beyond. As mentioned earlier, resonance-energy transfer (RT) and vibrational−rotational (VR) contributions which are difficult to model theoretically (and which are expected to be important in liquid nitrogen[12,21,22]) can be included in a simulation.

The simulations reported here reveal several unusual results. It is found that the experimental result of Clouter and Kiefte (on the pronounced insensitivity of the vibrational phase relaxation of the nitrogen fundamental to the change in thermodynamic conditions) can originate from a competition between the density relaxation and the resonant energy transfer terms. The dephasing relaxation rate is found to increase sharply near the critical point because of a sharp increase in the contribution of the vibration−rotation coupling. The results obtained here show that $\langle\Delta\omega_{10}(t)\ \Delta\omega_{10}(0)\rangle$ decay behavior is strongly Gaussian, with a small exponential tail in the long times. However, in accordance with the Kubo−Oxtoby theory, $\langle Q(t)\ Q(0)\rangle$ is found to be largely exponential *for the fundamental* for all the state points studied. In addition, the frequency modulation and the normal coordinate time correlation function (tcf) decay time scales are well separated. The extent of separation reduces as the system approaches the critical point and the Gaussian component in the initial decay of $\langle Q(t)\ Q(0)\rangle$ becomes more substantial. For higher overtones (third and above), the separation of time scales between the frequency modulation and the normal coordinate time correlation functions disappear near the critical point and in the supercritical fluids. This leads to an increased subquadratic quantum number dependence as the critical point is approached. Given the intense current interest in supercritical fluids, the above predictions should be tested against experiments. Limited subquadratic dependence is observed in the denser liquid states at higher overtones. Also, investigations on the density−temperature dependence of the overtone dephasing rate reveal an interesting crossover behavior, pronounced for higher overtones, in the liquid−gas phase transition region.

The above study raises an interesting question about the mode of determining the homogeneity of a Raman line shape. The usual criterion one employs (referred to here as Kubo−Oxtoby) is that the root-mean-square fluctuation of the frequency gap times the correlation time should be sufficiently less than unity. However, in the absence of a clear separation of time scales between the frequency modulation time correlation function and the normal coordinate time correlation function, this criterion seems to lose its meaning because one can obtain a Gaussian line shape even when the above condition is satisfied.

It should be pointed out that while the results reported here successfully reproduce the experimentally observed trends surprisingly well and are in semiquantitative agreement with the experimental results, the agreement is *not* quantitative for several state points, despite extensive simulations that we have carried out. We attribute this failure to the following factors. First, many terms of varying strengths contribute, some of which involve cross-correlations. It is notoriously difficult to estimate them correctly. Second, we have used the same pair potential for all the thermodynamic state points. This might be unreasonable because simulations have been carried out over large variations of temperature and density. Third, high-temperature simulation runs might involve a considerable amount of error as the molecular dynamics is extremely rapid in such cases. Fourth, we have neglected the quadrupolar interactions among the nitrogen molecules. While the simulations of both Cheung and Powles[35] and of Oxtoby and co-workers[21,22] indicate that this is not a serious approximation in the liquid phase and the gas phase, it can easily change the total dephasing rate by 5−10%.

The organization of the paper is as follows. Section 2 gives a theoretical discussion. The simulation details are presented in section 3. The results and discussion are presented in section 4. The paper concludes with a brief summary in section 5.

2. Theoretical Discussion: Inclusion of Resonance Energy Transfer and Vibrational−Rotational Contributions

The potential Hamiltonian for the vibrating mode (*Q*) was assumed to be of the following anharmonic form:

$$H_{\mathrm{vib}} = (1/2)\mu\omega_0{}^2Q^2 + (1/6)fQ^3 \quad (4)$$

where μ is the reduced mass, ω_0 is the vibrational frequency, and f is the anharmonic force constant.

If V is the oscillator-medium interaction potential, then using perturbation theory, one finds the following expression for thefluctuation in overtone frequency gap, $\Delta\omega_{n0}(t)$:[1,22]

$$\hbar\Delta\omega_{n0}(t) = (Q_{nn} - Q_{00})\left(\frac{\partial V}{\partial Q}\right)_{Q=0}(t) + \frac{1}{2}((Q)_{nn}{}^2 - (Q)_{00}{}^2)\left(\frac{\partial^2 V}{\partial^2 Q}\right)_{Q=0}(t) + Q_{n0}{}^2\sum_{j\neq i}\left(\frac{\partial^2 V}{\partial Q_i \partial Q_j}\right)_{Q=0}(t) + \ldots \quad (5)$$

In the estimation of $\Delta\omega_{n0}(t)$, only the first three terms were considered, neglecting the higher order terms. This is usually omitted in the theoretical modeling. The first term is not zero for an anharmonic potential and actually makes the maximum contribution to dephasing in several cases.[3,14] In the case of N_2,[14,21,36] this term is the more important one. The third term accounts for the resonance-energy transfer (RT) contribution. When anharmonicity is included, then one finds, using perturbation theory, the following expressions for the matrix elements of eq 5:

$$Q_{nn} - Q_{00} = \frac{n\hbar(-f)}{2\mu^2\omega_0{}^3}; \quad (Q)_{nn}{}^2 - (Q)_{00}{}^2 \simeq \frac{n\hbar}{\mu\omega_0}; \quad Q_{n0}{}^2 \simeq \delta_{n1}\frac{\hbar}{2\mu\omega_0} \quad (6)$$

where only the lowest order term has been retained in each case. In the above, n is the quantum number, $\hbar = h/2\pi$ where h is Planck's constant, μ is the reduced mass, ω_0 is the vibrational frequency, and δ_{n1} is the Kronecker delta. Thus, eq 5 can be written, for the ith molecule, as

$$\hbar\Delta\omega^i_{n0}(t) = \frac{n\hbar(-f)}{2\mu^2\omega^3}F^i_{1Q} + \frac{n\hbar}{2\mu\omega_0}F^i_{2Q} + \delta_{n1}\frac{\hbar}{2\mu\omega_0}{}^{1/2}\sum_{i\neq j}F^{ij}_3 \quad (7)$$

where the meaning of the force terms and the equations can be obtained by comparing eq 7 with eqs 5 and 6. Unless stated explicitly, the superscript i is not used in the frequency and the force terms in the subsequent discussions.

While the atom−atom (AA) contributions are given by eq 7, the vibration−rotation (VR) contribution to the broadening of the line shape is given by[6,7]

$$\langle\Delta\omega_{n0}(t)\,\Delta\omega_{n0}(0)\rangle_{\mathrm{VR}} = (\Delta R_{n0}/\hbar I_{\mathrm{m}}r_{\mathrm{e}})^2\langle\Delta J^2(t)\,\Delta J^2(0)\rangle \quad (8)$$

where J is the angular momentum, I_{m} is the moment of inertia value at the equilibrium bond length, r_{e}, and μ is the reduced mass. $\Delta R_{n0} = (Q_{nn} - Q_{00}) - 3(Q^2_{nn} - Q^2_{00})/2r_{\mathrm{e}}$ where $(Q_{nn} - Q_{00})$ and $(Q^2_{nn} - Q^2_{00})$ are the quantum mechanical expectation values of the bond length displacement and its square corresponding to the nth level given by eq 6.

As in earlier works,[6,7] we use

$$\langle\Delta J^2(t)\,\Delta J^2(0)\rangle = \langle J^2(t)\,J^2(0)\rangle - \langle J^2\rangle^2 \quad (9)$$

$\langle\Delta J^2(t)\,\Delta J^2(0)\rangle$ can be directly obtained from simulations. Note that this correlation function can be highly nonexponential in the short time scale,[6] particularly in dense liquids.[14] This again, like other nonexponential dephasing mechanisms, could significantly alter the n^2 dependence of the rate.

Neglecting the cross-correlation between the vibrational−rotational term and the atom−atom force terms, the total frequency time correlation function is written as

$$\langle\Delta\omega(t)\,\Delta\omega(0)\rangle_{n0} = \langle\Delta\omega_{n0}(t)\,\Delta\omega_{n0}(0)\rangle_{\mathrm{VR}} + \langle\Delta\omega_{n0}(t)\,\Delta\omega_{n0}(0)\rangle_{\mathrm{AA}} \quad (10)$$

where subscripts VR and AA represent the vibration−rotation and atom−atom contributions, respectively, to the dephasing.

The dephasing time ($\tau^{\Delta\omega}_{vn}$) for the nth level is usually defined using the frequency modulation tcf as[1]

$$(\tau^{\Delta\omega}_{vn})^{-1} = \int_0^\infty\langle\Delta\omega(t)\,\Delta\omega(0)\rangle_{n0}\,\mathrm{d}t \quad (11)$$

The presence of n in the contributions of F_{1Q} and F_{2Q} (which are usually more important) in eq 7 is the reason why the vibrational dephasing rate is usually assumed to exhibit the quadratic n dependence. However, as argued earlier, the dephasing time is given by the normal coordinate tcf and *not* the frequency modulation tcf. While $\langle\Delta\omega(t)\,\Delta\omega(0)\rangle_{n0}$ may have an n^2 dependence, the average dephasing rate ($\langle\tau_{vn}\rangle^{-1}$) obtained using eq 1 can show subquadratic dependence because, as mentioned earlier, $\langle Q(t)\,Q(0)\rangle_{n0}$ is expected to be biphasic with a Gaussian decay at short times followed by an exponential decay at longer times.[6,7,14] Assuming an exponential $\langle Q(t)\,Q(0)\rangle_{n0}$ decay, τ_{vn} can be obtained directly either by integrating the frequency modulation tcf or by eq 1.[1,14]

Dephasing mechanisms can be homogeneous (due to rapid modulation effects) or inhomogeneous (due to slow modulation effects). Using the frequency modulation tcf, one can also verify whether the dephasing mechanism is homogeneous or inhomogeneous. This can be done as follows.[3,21] Let τ_{cn} be the average frequency correlation decay time for the nth overtone defined as

$$\tau_{cn} = \int_0^\infty\frac{\langle\Delta\omega(t)\,\Delta\omega(0)\rangle_{n0}}{\langle\Delta\omega_{n0}(0)\,\Delta\omega_{n0}(0)\rangle}\,\mathrm{d}t \quad (12)$$

If the frequency fluctuations are weak enough and τ_{c} short enough such that

$$\langle\Delta\omega_{n0}{}^2(0)\rangle^{1/2}\tau_{cn} \ll 1 \quad (13)$$

then the Raman spectrum can be said to be homogeneously broadened or in the motional narrowing limit. On the other hand, if

$$\langle\Delta\omega_{n0}{}^2(0)\rangle^{1/2}\tau_{cn} \gg 1 \quad (14)$$

the spectrum is inhomogeneously broadened.

If a Raman spectrum is homogeneously broadened, $\langle\Delta\omega(t)\,\Delta\omega(0)\rangle_{n0}$ can be calculated by averaging over all molecules.[3,21] On the other hand, if the spectrum is inhomogeneously broadened, selective averaging of $\langle\Delta\omega_{n0}(t)\,\Delta\omega_{n0}(0)\rangle$ would be carried out over those molecules for which $\omega_{n0} + \omega_i(0)$ lies close to a given frequency ω.[3,21] In the case of liquid N_2, eq 13 is valid,[21,33] so that the added complications of inhomogeneous broadening need not be considered.

We have already remarked that the above Kubo−Oxtoby criterion does not remain unambiguous in the absence of a clear

separation of time scales between the frequency modulation time correlation function and the normal coordinate time correlation function. In particular, while the criterion for homogeneity (eq 13) can be satisfied, the line shape can still be Gaussian.

3. Simulation Details

Microcanonical (NVE) molecular dynamics simulations were carried out at different state points of N_2 ranging from the melting point (also the triple point of N_2) through the boiling point and the critical point. The system of 256 N_2 diatomic particles was enclosed in a cubic box, and periodic boundary conditions were used. In their work, Cheung and Powles[35] have reported little difference in the various thermodynamic properties between a 256- and 500-molecule system. Starting from an initial fcc lattice configuration, the system was allowed to equilibrate for 30 000 or so time steps. The unit of time, τ, is $\sqrt{(m\sigma^2/\epsilon)}$ with m the mass of the molecule which is calculated to be equal to 3.147 ps. After a few preliminary test runs, suitable sampling time intervals of 0.0002 (for high-density or high-temperature runs) and 0.0004 (for medium-density and medium-temperature runs) were chosen for the studies at different state points. The study of N_2 at close to its boiling point was already presented in ref 33, where emphasis was only on the subquadratic quantum number dependence. It is also presented in this paper as part of the temperature- and density-dependent studies.

It is to be pointed out that high-temperature simulation studies (such as near critical point (CP) and beyond) might involve a considerable amount of error despite the use of a very small time step (and, so, very long runs), as the molecule dynamics is extremely rapid in such cases. Also, the high-temperature simulation runs are likely to be susceptible to system size, though, as mentioned earlier, little difference in the various liquid thermodynamic properties has been reported between a 256- and 500-molecule system.[35]

The thermodynamic state of the system can be expressed in terms of the reduced density of $\rho^* = \rho\sigma^3$ and a reduced temperature of $T^* = k_B T/\epsilon$ (the density is expressed in number of molecules per unit volume times σ^3 where σ is the Lennard-Jones diameter of the molecule and the temperature in units of ϵ/k_B where k_B is the Boltzmann constant). Cheung and Powles[35] had earlier studied liquid N_2 at different state points using MD simulations. Most of the thermodynamic state points chosen for the work presented here have been taken from their study.

As mentioned earlier, a quantum mechanical perturbation theory for the vibrational motion (Q) has been used here and thereby expressed the dephasing rate in terms of autocorrelation and cross-correlation functions of F_{1Q}, F_{2Q}, and F_{3Q}. Since these are estimated at $Q = 0$ (see eq 5), they may be obtained from simulations of rigid molecules.

For the intermolecular potential energy (V_{ij}) between two molecules i and j, the following site−site Lennard-Jones type was employed.

$$V_{ij} = \sum_{a,b}^{1,2} V(r_{iajb}) \tag{15}$$

where $V(r_{iajb})$ is the Lennard-Jones atom−atom potential with

$$V_{iajb} = 4\epsilon_{iajb}\left[\left(\frac{\sigma_{iajb}}{r_{iajb}}\right)^{12} - \left(\frac{\sigma_{iajb}}{r_{iajb}}\right)^{6}\right] \tag{16}$$

where r_{iajb} (or r_{iajb}) is the distance between ath atom on molecule i and bth atom on molecule j, ϵ_{iajb} is the Lennard-Jones well-depth potential, and σ_{iajb} is the Lennard-Jones diameter. For dissimilar a and b atoms, ϵ_{iajb} and σ_{iajb} are estimated from those of the similar spheres through the combining rule $\epsilon_{iajb} = \sqrt{\epsilon_{aa}\epsilon_{bb}}$ and $\sigma_{iajb} = (\sigma_{aa} + \sigma_{bb})/2$.[37]

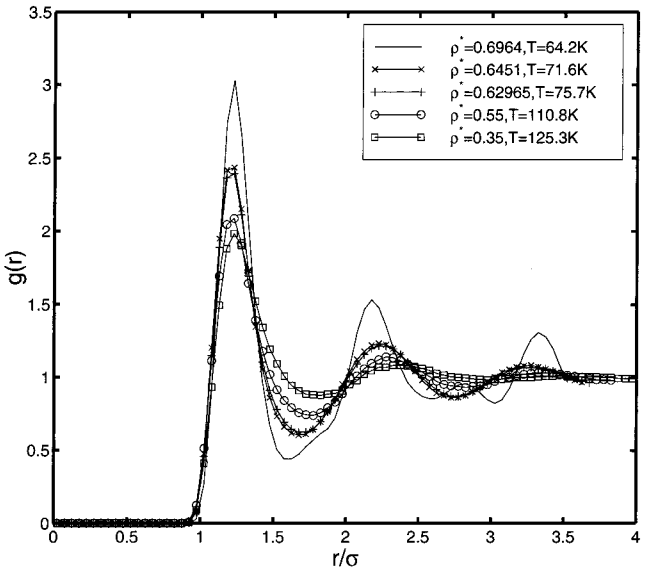

Figure 1. Simulated pair-correlation functions for the nuclei N^1 and N^2 of N_2, g_{N^1} and g_{N^2}, and for its molecular center, g_{N^2}, obtained at different state points: $(\rho^*,T) = (0.6964,64.2K)$ for TP, (0.6451,71.6K), (0.62965,75.7) for BP, (0.5983,T=89.5), (0.55,110.8K), (0.35,125.3K) for CP. The decrease in the peak heights shows the evolution of the system as it moves from the dense solid phase toward the gas phase. Distinct "shoulder" regions appear in the range $1.5 < r^* < 2.0$ near the melting point (MP) indicating structure formation. $r^* = r/\sigma$ where σ is equal to 3.31 Å.

For the above potential form, the quantities F^i_{1Q}, F^i_{2Q}, and F^i_{3Q} are to be calculated in order to obtain the AA contribution to the frequency modulation value as described in eq 7. Reference 14 describes in detail the procedure to obtain the above-mentioned quantities.

4. Results and Discussion

The liquid structure is characterized by a set of distribution functions for the atomic positions, the simplest of which is the pair distribution function, $g(r)$. This function gives the probability of finding a pair of atoms a distance r apart, relative to the probability expected for a completely random distribution at the same density. $g(r)$ is formally defined as

$$g(r) = \frac{1}{\rho^2}\left\langle \sum_i \sum_{j\neq i} \delta(\mathbf{r}_i)\,\delta(\mathbf{r}_j - \mathbf{r})\right\rangle = \frac{V}{N^2}\left\langle \sum_i \sum_{j\neq i} \delta(\mathbf{r}_i)\,\delta(\mathbf{r}_j - \mathbf{r})\right\rangle \tag{17}$$

where V and N are the volume and the number of molecules in the system, respectively.

As the structure of a molecular fluid can be described using the pair distribution function $g(r)$, the evolution of the system from the melting point (MP) to the CP was monitored using $g(r)$. In Figure 1, the pair correlation of N_2 molecular center ($g_{N_2}(r)$) obtained at different state points are shown. The decrease in the peak heights leading to a less structured and more homogeneous distribution as the state of the system moves from close to the melting point to the gas phase clearly reveals the evolution from a dense liquid state to a gaseous state. At temperatures higher than the one close to the melting point (64.2 K), $g_{N_2}(r)$ is effectively unity at distances beyond 3.0σ, indicating a virtually uniform distribution. Even near the melting

TABLE 1: Dynamical Properties—Relaxation Time (τ_{vel}) and Diffusion Coefficient (D) Obtained from the Velocity Correlation Function and the Rotational Correlation Times for the First and Second Ranks—for Liquid Nitrogen at Various State Points

ρ^*	T (K)	D (10^9 m^2/s)	τ_{vel} (ps)	τ_{1R} (ps)	τ_{2R} (ps)	τ_{1R}/τ_{2R}
0.6964	64.2	10^{-6}		0.43182	0.22884	1.887
0.6452	71.6	1.859	0.093	0.528	0.273	1.934
0.62965	75.7	2.27	0.103	0.446	0.237	1.882
0.5983	89.5	4.084	0.167	0.3952	0.21	1.883
0.55	110.8	6.857	0.218	0.262	0.167	1.567
0.35	125.3	17.96	0.512	0.195	0.192	1.015
0.2	149.2	147.4	1.102	0.129	0.26	0.49

point, the departure from uniformity beyond 3.2σ is about 5%. This is probably sufficient to justify the cutoff imposed at 3.2σ in evaluating the forces.

In the case of N_2 at near the MP, a distinct "shoulder" region appears in the region $1.5 < r^* < 2.0$. A similar feature was observed in the case of CH_3I, as found in our earlier study.[14] Moreover, an additional peak is observed near MP in the region $2.5 < r^* < 3.0$, clearly indicating structure formations. Such shoulders and additional peaks might be due to orientational ordering as the N_2 molecules are not spherically symmetric and their intermolecular interactions depend on the relative orientations of pairs of molecules as well as on the distance between the molecular centers. The extent and type of correlations of molecular orientations, particularly those of near neighbors, can be expected to influence strongly the degree of overlap of the hard repulsive cores of the molecules, and so have significant effects on the energies of fluid and solid phases. Such correlations will also affect the ways in which the molecules can be packed together in both phases. For centrosymmetric molecules such as N_2, the most probable orientations would be of the following types: perpendicular configuration in which the molecules are perpendicular to each other and parallel configuration in which the molecules lay side by side.[38] Melting data for N_2 suggests that there probably is greater local orientational order in the dense fluid phases of N_2 than in its solid phase near melting.[39] Earlier simulations by Cheung and Powles have also reported structure factor results that indicate structure formation in the long range near the melting point.[35]

4.1. Translational Motions. The translational motions are usually characterized using the velocity and force tcfs. These functions are defined as follows.

$$C_v(t) = \frac{\langle \mathbf{v}(t)\cdot\mathbf{v}(0)\rangle}{\langle \mathbf{v}(0)\cdot\mathbf{v}(0)\rangle} \tag{18}$$

$$C_F(t) = \frac{\langle \mathbf{F}(t)\cdot\mathbf{F}(0)\rangle}{\langle \mathbf{F}(0)\cdot\mathbf{F}(0)\rangle} \tag{19}$$

where **v** and **F** are the velocity and the force of the molecular center of mass, respectively.

The diffusional coefficient D can also be obtained using the velocity tcf and is given as follows.

$$D = \frac{1}{3}\int_0^\infty \langle \mathbf{v}(t)\cdot\mathbf{v}(0)\rangle = \frac{\langle v^2(0)\rangle \tau_{vel}}{3} \tag{20}$$

The D values obtained from simulations are given in Table 1 and simulated $C_F(t)$ obtained at various state points are shown in Figure 2. $C_F(t)$ profiles show a pronounced Gaussian in the initial time scale followed by slowly relaxing decay, characteristics rather similar to those obtained using MCT.[14] Also, these correlations clearly reflect the cage effects (due to the rebound of the molecule in question against the cage formed by its nearest neighbors[40]) that are associated with dense fluids with a deep minimum at denser state points in the simulated

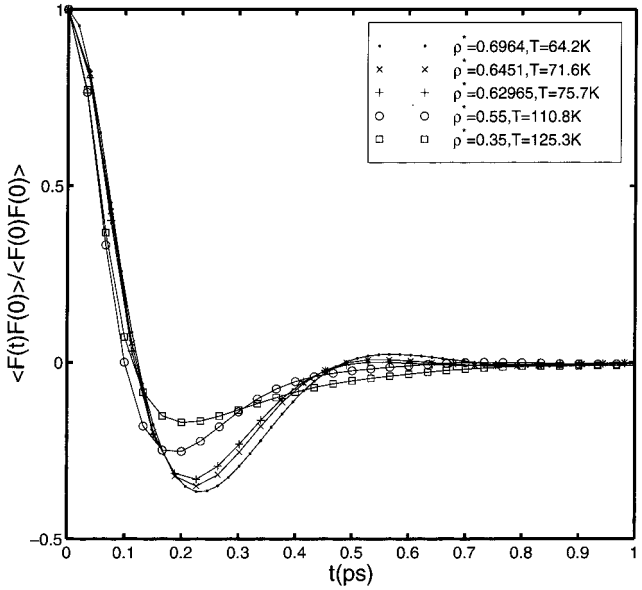

Figure 2. MD simulated normalized force correlation functions for the N_2 molecular center (COM) obtained at different state points of liquid N_2: $(\rho^*,T) = (0.6964,64.2\text{K})$ for TP, (0.6451,71.6K), (0.62965,-75.7) for BP, (0.5983,T=89.5), (0.55,110.8K), (0.35,125.3K) for CP. The correlations clearly exhibit a quickly relaxing component in the initial time scale followed by a slower one. At higher densities, the decay shows a deep negative minimum indicating cage effects.

force correlation profiles. Such effects have been explained in terms of the existence of a loose structure or "cage" of neighboring molecules with a lifetime comparable to τ_{vel}, the relaxation time of the velocity tcf. τ_{vel} values obtained from simulations are given in Table 1.

4.2. Orientational Motions. As diatomics are involved in this study, characterizations regarding orientational motions are also presented here. These are important in understanding the vibration−rotation coupling which has been found to play an important role in the high-temperature gas phase. The molecular axis orientational correlation functions of the first and second ranks, C_{1R} and C_{2R}, respectively, are defined as

$$C_{1R}(t) = \langle P_1(\mathbf{u}(t)\cdot\mathbf{u}(0))\rangle = \langle \mathbf{u}(t)\cdot\mathbf{u}(0)\rangle \tag{21}$$

$$C_{2R}(t) = \langle P_2(\mathbf{u}(t)\cdot\mathbf{u}(0))\rangle = \frac{\langle 3(\mathbf{u}(t)\cdot\mathbf{u}(0))^2 - 1\rangle}{2} \tag{22}$$

where **u** is the unit vector along the diatomic axis.

The simulated molecular axis orientational correlation functions of the first C_{1R} and second C_{2R} ranks are shown in Figures 3 and 4, respectively. The estimated correlation times for the first and second ranks are also shown in Table 1. For liquids, the relaxation of C_{2R} is faster and the ratio of τ_{1R}/τ_{2R} is normally between 3.0 and 1.0.[41] The estimated ratios as given in Table 1 lie in this range for all the temperatures below and up to the critical point. For the state point in the gas phase ($\rho = 0.2$ and

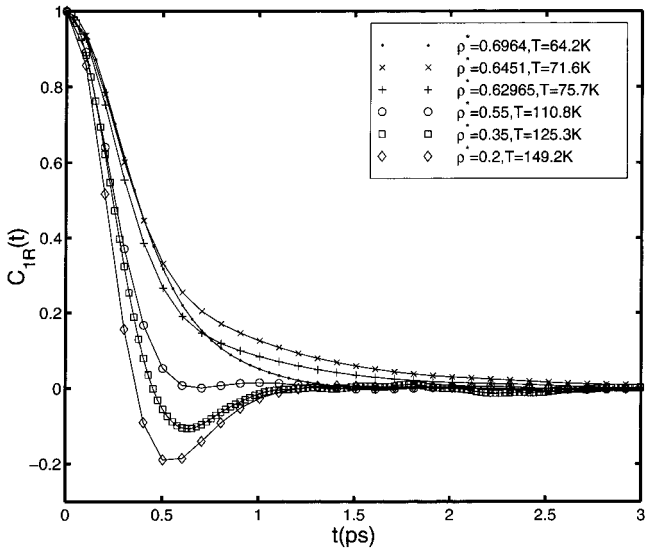

Figure 3. MD simulated orientational correlation function for the first rank ($C_{1R}(t)$) of molecular N−N axis obtained at different state points of liquid N_2: (ρ^*,T) = (0.6964,64.2K) for TP, (0.6451,71.6K), (0.62965,75.7) for BP, (0.5983,T=89.5), (0.55,110.8K), (0.35,125.3K) for CP, (0.2,149.2K).

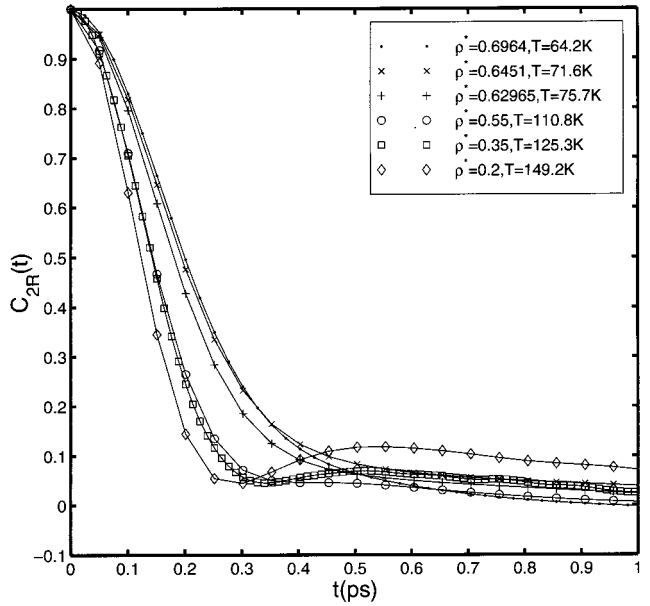

Figure 4. MD simulated orientational correlation function for the second rank ($C_{2R}(t)$) of molecular N−N axis obtained at different state points of liquid N_2: (ρ^*,T) = (0.6964,64.2K) for TP, (0.6451,71.6K), (0.62965,75.7) for BP, (0.5983,T=89.5), (0.55,110.8K), (0.35,125.3K) for CP, (0.2,149.2K).

T = 149.2 K), the ratio τ_{1R}/τ_{2R} is found to be less than 1. This is in accordance with the predicted orientational relaxation behavior in the gas phase.[42] In the limit $t \rightarrow \infty$, C_{1R} goes to zero but C_{2R} tends to a constant value (equal to 1/4 for a system of noninteracting rigid rotors). The precursor of this effect is already seen in the very high temperature gas phase. Also, typical characteristerics of C_{2R} relaxation behavior such as a faster initial decay of C_{2R} than that of C_{1R} in the presence of interactions (in the denser liquid states) has been observed. We have discussed elsewhere[41] that higher (than 1) rank orientational correlation functions often do not approach the diffusive behavior because these correlations probe high-frequency friction of the medium and the latter is often insufficient to render rotation diffusive.

TABLE 2: Simulated Average Frequency Shifts, Mean Square Frequency Modulation Value, and Frequency Modulation Correlation Time for N−N Stretching in Liquid N_2 at Various State Points

ρ^*	T (K)	$\langle\Delta\omega\rangle$ (cm^{-1})	$\langle\Delta\omega^2(0)\rangle_{10}^{1/2}$ (ps^{-1})	τ_{c1} (ps)	$\langle\Delta\omega^2\rangle_{10}^{1/2}\tau_{c1}$
0.6964	64.2	5.17	0.35	0.088	0.031
0.6451	71.6	1.91	0.283	0.153	0.43
0.62965	75.7	1.90	0.292	0.126	0.036
0.5983	89.5	1.80	0.315	0.150	0.047
0.55	110.7	1.55	0.34	0.132	0.045
0.35	125.3	0.82	0.28	0.197	0.055

4.3. Vibrational Dephasing in Nitrogen Ranging from Triple Point to Critical Point and Beyond. The frequency modulation time correlation function and the dephasing line width (proportional to the dephasing rate) have been calculated for several thermodynamic state points ranging from the triple point to the critical point and beyond. In the following we present the numerical results on dephasing.

For the fundamental, the average frequency shift ($\langle\Delta\omega_{10}\rangle$), mean square frequency fluctuation value ($\langle\Delta\omega^2(0)\rangle_{10}$ value), and the frequency modulation correlation time (τ_{c1}) have been calculated at the different state points studied. The estimated mean square frequency fluctuation value ($\langle\Delta\omega_{10}^2(0)\rangle$) and the frequency modulation correlation time τ_{c1} for the different state points are shown in Table 2. As expected, the frequency shift was found to increase as the system moves from the gas phase (CP) to the solid phase (TP) due to stronger intermolecular interactions in the denser liquid phase. However, the sign of the shift is found to be not predicted properly.[9] For example, near the BP, the simulated shift is about 1.9 ± 0.1 cm^{-1} and the experimentally reported shift value is −1.7 cm^{-1}. Such prediction of the wrong sign for the gas-to-solution frequency shift could be due to the neglect of changes in bond polarizability upon vibrational excitation[22,43,44] and the neglect of cross-correlation effects between vibration−rotation contributions and atom−atom contributions.[44] The product of $\langle\Delta\omega^2(0)\rangle_{10}^{1/2}$ and τ_{c1} has been found to be significantly less than unity for all the state points, so the dephasing process can be considered as homogeneous.[3,21] The simulated frequency modulation time correlation function (tcf) ($\langle\Delta\omega_{10}(t)\,\Delta\omega_{10}(0)\rangle$) decay is found to be Gaussian at all state points studied as shown in Figure 5. The normal coordinate tcf ($\langle Q(t)\,Q(0)\rangle_{10}$) is, in contrast, largely exponential in the liquid phase, as shown in Figure 6. Moreover, the time scales of the above two decays are well separated. However, this separation decreases as the thermodynamic state moves toward the critical point and beyond. Also, the Gaussian component of $\langle Q(t)\,Q(0)\rangle_{10}$ in the initial time scale is found to become more substantial as the system approaches the critical point.

The dephasing line width (equal to $2/\tau_{v1}$ where $\tau_{v1} = \int_0^\infty\langle Q(t)\,Q(0)\rangle_{10}$) for the fundamental obtained for several thermodynamic state points ranging from the triple point to the critical point and also along the critical isochore are as shown in Figure 7. *The simulated results from the TP to the CP show good qualitative agreement with the experimental observations.*[9,45] It is indeed remarkable that the line width remains more or less constant from the triple point to within 10 K below the critical point. We found that this insensitivity actually arises from a cancellation of two effects in this region: an increase in the mean square frequency value $\langle\Delta\omega_{10}^2(0)\rangle$ (i.e., due to an increase in AA contributions, RT in particular, as a result of stronger intermolecular interactions in the denser states) with a corresponding decrease in the correlation time τ_{c1} as the system moves toward the triple point. However, the study along the

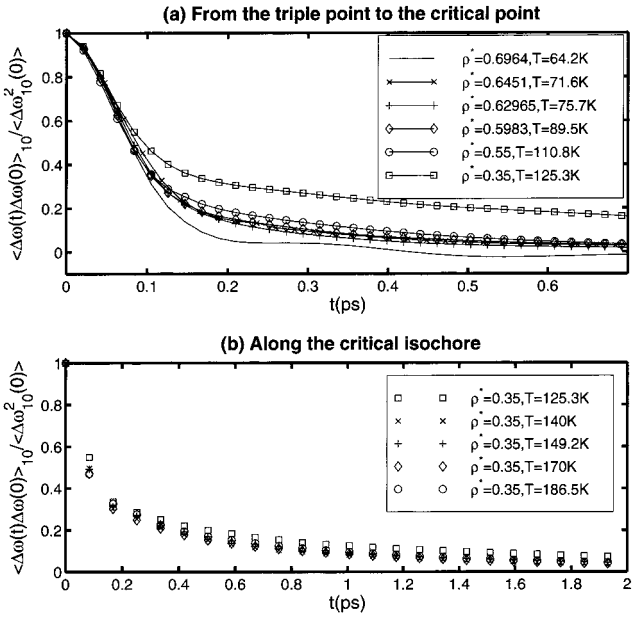

Figure 5. MD simulated normalized frequency modulation time correlation function for the fundamental in N_2 obtained at different state points (a) from the triple point to the critical point: $(\rho^*,T) = (0.6964,64.2\text{K})$ for TP, (0.6451,71.6K), (0.62965,75.7) for BP, (0.5983,T=89.5), (0.55,110.8K), (0.35,125.3K) for CP; (b) along the critical isochore: (ρ^*,T) = (0.35,125.3K), (0.35,140K), (0.35,149.2K), (0.35,170K), (0.35,186.5K). The plot shows a clear Gaussian component in the initial time scale followed by a slower decay.

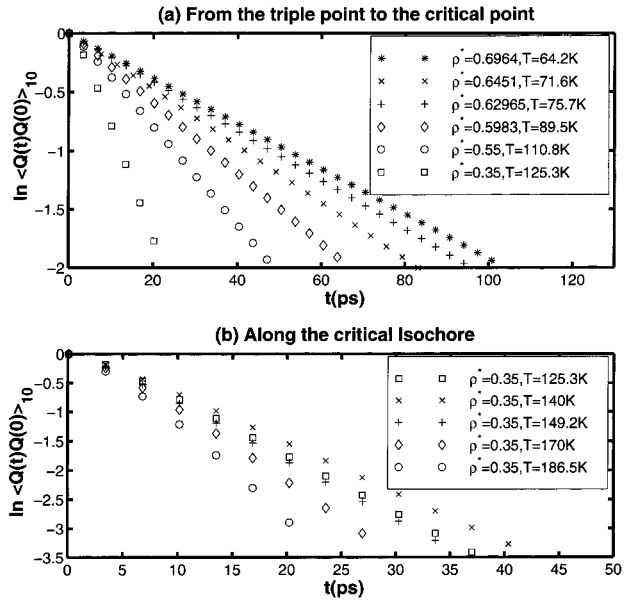

Figure 6. Simulated plots of ln $\langle Q(t)\ Q(0)_{10}\rangle$ vs t for N_2 obtained at different state points. (a) From the triple point to the critical point: $(\rho^*,T) = (0.6964,64.2\text{K})$ for TP, (0.6451,71.6K), (0.62965,75.7) for BP, (0.5983,T=89.5), (0.55,110.8K), (0.35,125.3K) for CP. (b) Along the critical isochore: (ρ^*,T) = (0.35,125.3K), (0.35,140K), (0.35,149.2K), (0.35,170K), (0.35,186.5K). The results clearly show largely exponential behavior in all the cases. The Gaussian component in $\langle Q(t)\ Q(0)\rangle_{10}$ relaxation increases and the separation of the relaxation time scales of $\langle \Delta\omega_{10}(0)\ \Delta\omega_{10}(0)\rangle$ and $\langle Q(t)\ Q(0)\rangle_{10}$ reduces as the system moves toward the gas phase (critical point).

critical isochore does not reveal perfect agreement with the experimental results. Also, there is quite a steep rise in the simulated line width beyond 140 K. This discrepancy could partly be due to errors involved in very high temperature simulations.

As one proceeds from the low temperature liquid to the high

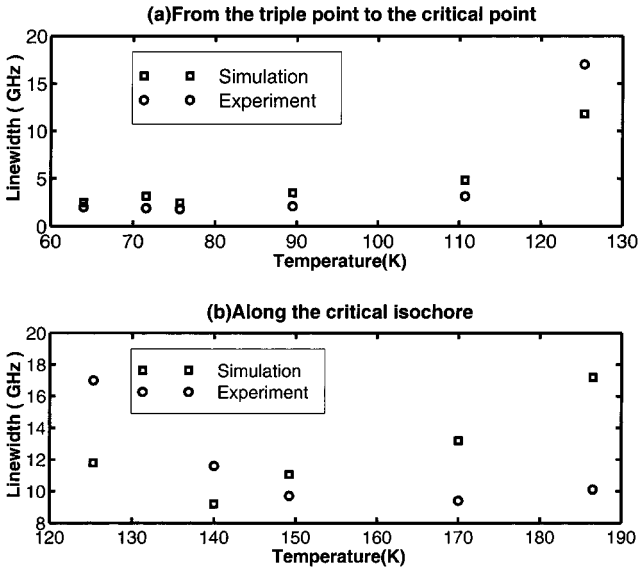

Figure 7. Simulated dephasing line width estimates (squares) for the fundamental of the N−N stretching in liquid N_2 at different state points: (a) Ranging from the triple point (TP) to the critical point (CP): $(\rho^*,T) = (0.6964,64.2\text{K})$ for TP, (0.6451,71.6K), (0.62965,75.7) for BP, (0.5983,T=89.5), (0.55,110.8K), (0.35,125.3K) for CP; (b) along the critical isochore: (ρ^*,T) = (0.35,125.3K), (0.35,140K), (0.35,149.2K), (0.35,170K), (0.35,186.5K). The results show a rapid increase of the line width toward the critical point (CP) due to a large vibrational−rotational contribution near the critical region. The experimental results (dots) reported by Clouter and Kiefte in ref 9 (from the TP to CP) and by Chesnoy in ref 45 (along the critical isochore) are also shown.

temperature gas phase, it is not clear whether to consider the system in the motional narrowing limit, because the VR line width becomes very broad and Gaussian. Thus, even when the relaxation satisfies the homogeneity criteria (eq 13), we still have a non-Lorentzian line shape. This is against the conventional wisdom from the Kubo−Oxtoby theory that the line shape is in the motional narrowing limit when the condition of homogeneity is satisfied. This conventional wisdom becomes inadequate when the separation of time scales of the frequency modulation and the normal coordinate time correlation functions disappear. This will be important both for nitrogen dephasing in the supercritical state and for overtone dephasing of C−I stretch in methyl iodide.

The effects of the resonant transfer and the vibration−rotation coupling on dephasing were also studied by selectively eliminating their individual contributions. These additional dephasing mechanisms might increase or decrease the dephasing time because the sign of their contribution is determined by the cross-correlation terms. However, *in all cases, both RT and VR contributions were found to decrease the overall dephasing time*. The estimated values of the individual contributions in addition to the total are given in Table 3.

When only the atom−atom contributions are considered, the mean square value of the frequency fluctuation for fundamental, $\langle \Delta\omega_{10}{}^2\rangle$, reflects roughly the extent of combined influence of the collisional, repulsive, and attractive interactions to the friction on the bond (and, therefore, dephasing).[33] In the case of N_2, $\langle \Delta\omega_{10}{}^2\rangle$ is found to follow a non-monotonic dependence from the critical point to the triple point. This could be due to an intricate balance between the contributions of the repulsive, attractive, and collisional interactions to dephasing.

On the other hand, resonance-energy transfer (RT) contribution is found to increase with increasing density due to stronger

TABLE 3: Autocorrelation and Cross-Correlation Contributions to Dephasing from the Various Mechanisms ($D = F_{1Q} + F_{2Q}$, $R = F_{3Q}$, $V =$ VR, DR $= D + R$, DRV $= D + R + V$) and the Dephasing Time Obtained from Simulations for the First Overtone of the N−N Stretching in Liquid N_2

(a) At Different State Points Ranging from the Triple Point to the Critical Point

		$\langle\Delta\omega_{10}^2\rangle^{1/2}$ (ps^{-1})					τ_{c1} (ps)			τ_{v1}^Q (ps)	
ρ^*	T (K)	D	R	V	DR	DRV	D	DR	DRV	sim	expt
0.6964	64.2	0.25	0.21	0.08	0.34	0.35	0.086	0.079	0.088	119	127
0.6452	71.6	0.244	0.08	0.088	0.27	0.283	0.143	0.158	0.153	85.6	134
0.62965	75.7	0.254	0.077	0.099	0.273	0.292	0.13	0.128	0.126	110	150
0.5983	89.5	0.272	0.077	0.117	0.29	0.315	0.099	.095	0.150	76.8	128
0.55	110.8	0.30	0.081	0.14	0.322	0.34	0.101	0.106	0.132	55.85	86
0.35	125.3	0.223	0.044	0.15	0.24	0.28	0.124	0.121	0.197	22.8	14.5

(b) At Different Temperatures along the Isochore

		$\langle\Delta\omega_{10}^2\rangle$ (ps^{-2})			τ_{c1} (ps)				τ_{v1}^Q (ps)	
ρ^*	T (K)	D	DR	V	DRV	D	DR	DRV	sim	expt
0.35	125.3	0.05	0.056	0.022	0.079	0.124	0.121	0.196	22.8	14.5
0.35	140	0.06	0.069	0.033	0.094	0.096	0.093	0.405	29.3	23.3
0.35	149.2	0.068	0.077	0.039	0.12	0.09	0.088	0.39	24.4	27.8
0.35	170	0.079	0.089	0.046	0.13	0.083	0.081	0.43	20.4	28.6
0.35	186.5	0.09	0.1	0.57	0.157	0.077	0.075	0.52	15.7	26.7

intermolecular interactions among the closely spaced molecules. Similar experimental observations have been reported earlier for the polarized modes of N_2O in Xe.[46] The RT contribution, often considered small, is found to be close to 50% of the total near the melting point (also the triple point) and gradually decreases as one moves away from the melting point (MP). It should, however, be pointed out that for the case near the MP the equilibration did not satisfactorily lead to a homogeneous liquid state (as some "shoulder" regions[33] indicating structure formations were observed in the radial distribution function), and so the above estimate could involve some error as the system was still considered as homogeneous. Nevertheless, the qualitative trends appear to be consistent.

Vibration−rotation contributions are also found to be significant but not very large (about 15−25%) from the triple point to within 10 K from the critical point, in accordance with earlier theoretical observations by Brueck[12] for liquid N_2. However, the VR contributions become increasingly substantial as the system approaches the gas phase (toward the critical point) because of the increase in the molecular rotational kinetic energy with increase in temperature. The line width, therefore, was found to increase rapidly as the critical point was approached as shown in Figure 9 due to increasing rotational line width as the system approaches the gas phase. This explains the large line widths observed along the critical isochore ($\rho = \rho_c$), as found in the earlier experimental studies near gas−liquid critical points.[9,45]

Although the contribution of the vibration−rotation coupling term to overall dephasing is significant in the gas phase due to very high rotational kinetic energies of the molecule at high temperatures, the relaxation of the relevant time correlation function is found to be almost exponential, as shown in Figure 8, and relatively slower (of the order of a few picoseconds). This makes the decay of $\langle\Delta\omega_{10}(t)\ \Delta\omega_{10}(0)\rangle$ slower, as shown in Figure 5). On the other hand, overtone studies reveal substantial subquadratic dependence along the critical isochore as shown in Figure 9. This arises from an interesting interplay between the atom−atom and VR contributions. A large VR contribution enhances the value of the mean square frequency fluctuation, thereby reducing the overall decay time of $\langle Q(t)\ Q(0)\rangle_{10}$. This in turn decreases the separation of relaxation time scales between the $\langle\Delta\omega_{10}(t)\ \Delta\omega_{10}(0)\rangle$ and $\langle Q(t)\ Q(0)\rangle_{10}$ tcf's. On the other hand, the AA contribution renders the $\langle Q(t)\ Q(0)\rangle_{10}$ relaxation Gaussian in the short time scale. The contribution

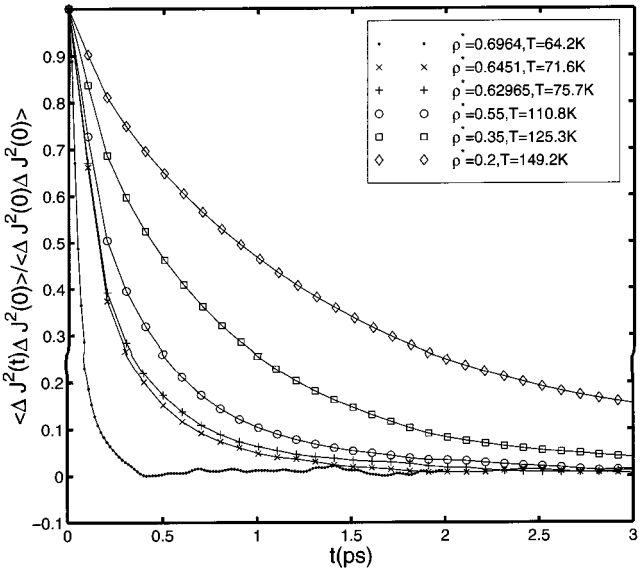

Figure 8. MD simulated normalized squared-angular momentum correlation function for the N_2 molecular center (COM) obtained at different state points: $(\rho^*,T) = (0.6964,64.2\text{K})$ for TP, (0.6451,71.6K), (0.62965,75.7) for BP, (0.5983,T=89.5), (0.55,110.8K), (0.35,125.3K) for CP. The relaxation becomes slower and increasingly exponential as the system moves toward the gas phase.

from the Gaussian component to $\langle Q(t)\ Q(0)\rangle_{10}$ in the initial time scale, therefore, becomes prominent near the critical point due to relatively faster relaxation of $\langle Q(t)\ Q(0)\rangle_{10}$, leading to a pronounced subquadratic dependence along the critical isochore.

It should be pointed out that critical point effects that involve long-range mechanisms such as collective density fluctuations or cluster formations are expected to complicate the system dynamics and contribute to the dephasing.[47−49] These effects may not be possible to fully accommodate in a finite small-sized system modeling such as in a simple simulation, although recent simulations in near-critical solution[48] have demonstrated that even a rather small simulation can yield an adequate description of the local solvation environment that most strongly influences the solute's spectroscopy. However, the extent of cluster effects may not be negligible.

It should also be pointed out that the determination of the extent of the role of the various dephasing mechanisms is quite likely to be sensitive to the simulation errors, more so in the

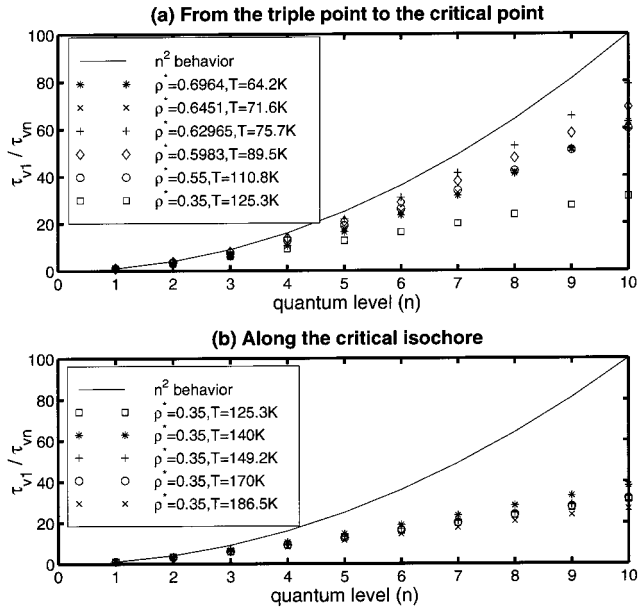

Figure 9. Plots of the ratio of the fundamental to the overtone vibrational dephasing times (τ_{v1}/τ_{vn}) plotted as a function of the quantum number n for N−N stretching in N_2 obtained at different state points: (a) Ranging from the triple point to the critical point: (ρ^*,T) = (0.6964,-64.2K) for TP, (0.6451,71.6K), (0.62965,75.7) for BP, (0.5983,T=89.5), (0.55,110.8K), (0.35,125.3K) for CP. (b) Along the critical isochore. The results show a highly subquadratic dependence near the critical point due to the increased Gaussian component in $\langle Q(t)\, Q(0)\rangle$ relaxation.

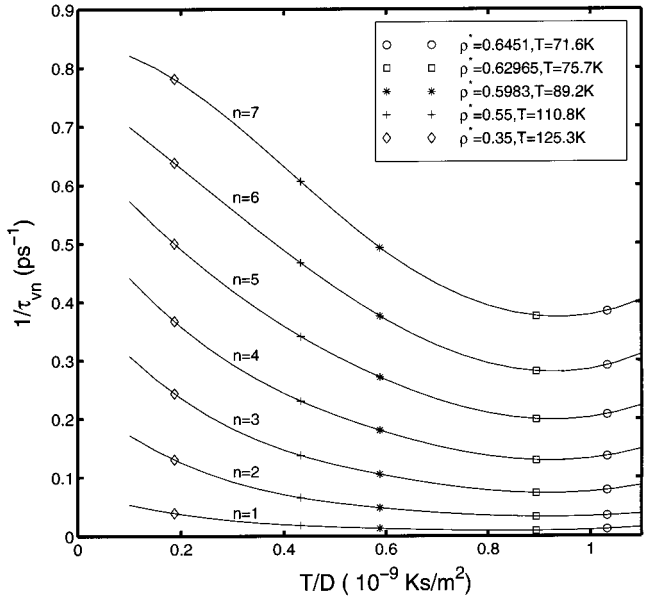

Figure 10. Plot of the overtone vibrational dephasing rates (τ_{vn}^{-1}) vs temperature/diffusion coefficient (T^*/D) for N−N stretching in N_2 obtained at different state points ranging from the triple point to the critical point: (ρ^*,T) =(0.6451,71.6K), (0.62965,75.7) for BP, (0.5983,T=89.5), (0.55,110.8K), (0.35,125.3K) for CP. The results show a clear crossover behavior near the liquid−gas phase transition point at $\rho^* = 0.5983$ and $T = 89.2$ K.

case of state points close to the phase transition regions. Nevertheless, the estimation of the dephasing times shows good qualitative agreement with the experimental observations.

4.4. Study of Density−Temperature−Viscosity Dependence of the Dephasing Rate. As mentioned earlier, most theoretical studies (which have not included the resonance-energy transfer and vibrational−rotational terms that have been shown to be significant) have predicted strong dependence of the dephasing rate on the viscosity of the liquid. The binary collision model[20] predicts a line width proportional to $\eta\rho^{-1}T$, the hydrodynamic theory[1] ηT, and Lynden-Bell's theory[24] $\eta\rho T^{-1}$. It is clear from the present work and from our earlier studies that the dephasing rate and its quantum number dependence are directly related to the dynamic friction (which has a biphasic structure). In fact, the hydrodynamic theory relates the dephasing directly to the friction. One then relates this friction to viscosity by using Stokes' expression. In view of the above, we investigated the overtone dephasing rate dependence on temperature (T)/diffusion coefficient (D) factor as the friction is related to T/D. The results as shown in Figure 10 reveal highly interesting behavior. Near $\rho^* = 0.5983$ and $T =$ 89.5 K (a state point which roughly represents the liquid−gas phase boundary), a crossover behavior in the dependence of rate on T/D is clearly observed. Similar behavior is also observed in dephasing rate vs *temperature* (T^*)/ρ^* as shown in Figure 11.

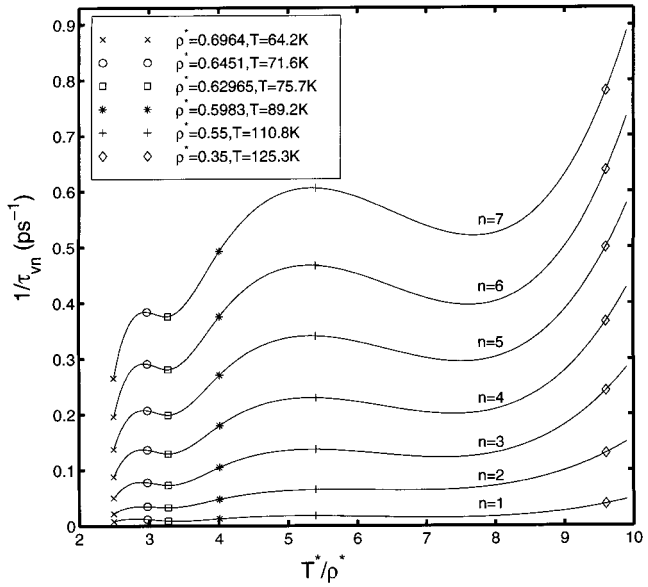

Figure 11. Plot of overtone vibrational dephasing rates (τ_{vn}^{-1}) vs temperature/density (T^*/ρ^*) for N−N stretching in N_2 obtained at different state points ranging from the triple point to the critical point: (ρ^*,T) = (0.6451,71.6K), (0.62965,75.7) for BP, (0.5983,T=89.5), (0.55,110.8K), (0.35,125.3K) for CP. The results show a clear crossover behavior near the liquid−gas phase transition point at $\rho^* = 0.5983$ and $T = 89.2$ K.

Figure 10 shows that in the region closer to the gas phase (higher temperature and low density) there is a nonlinear *decrease* of the rate with T/D indicating a total breakdown of the hydrodynamic theory in this region. This is as expected because in the gas phase the mechanism of dephasing is different from that in the liquid, as discussed above. On the other hand, in the liquid region involving temperatures below $T = 89.5$ K, there is a nearly *linear increase* of the rate with T/D, which indicates the emergence of the validity of the hydrodynamic theory in this region. Figure 11 shows a nonlinear dependence of the dephasing rate on the combination T^*/ρ^* for small values of the latter. This is the liquid region where non-IBC behavior is expected; the isolated binary collision (IBC) model is not expected to be vaild in the liquid. The same figure also shows the emergence of the IBC behavior in the gas phase. It is also interesting to note that the gas to liquid crossover behavior is more pronounced at higher overtones and, therefore, the phase transition is more sharply revealed at higher overtones. This, again, could be due to the strong dependence of higher-overtone dynamics to short-time relaxation behavior.

The above results of the MD simulation can be tested against experiments.

5. Conclusion

In this article results of extensive molecular dynamics (MD) simulations of vibrational dephasing of liquid nitrogen at several thermodynamic state points have been presented. The thermodynamic state points have been chosen to lie along the phase coexistence line from the triple point to the critical point (via the melting point) and beyond. In addition, two states have been chosen away from the coexistence—one in the normal liquid range and the other in the supercritical fluid state. Our reason to simulate the coexistence region is that the interesting and yet unexplained results of Clouter and Kiefte[9] are available in this region.

It is found that the time dependence of the frequency modulation time correlation function is strongly biphasic, with an initial ultrafast Gaussian component at all temperatures. Below the boiling point the decay of the normal coordinate time correlation function, $\langle Q(t)\, Q(0)\rangle$, on the other hand, is largely exponential and also the decay time scales of the frequency modulation and normal coordinate tcf's are well separated. However, the extent of this separation decreases rapidly as the system moves closer to the critical point. This results in an increasing subquadratic behavior near the critical point. Dephasing due to resonant-energy transfer was found to be significant in liquid N_2 at higher densities. On the other hand, vibration−rotation contribution was found to increase rapidly near the gas phase as the rotational kinetic energy of the molecules increases with temperature.

The simulations reported here seem to reproduce many of the anomalies observed in experiments and provide quantitative explanation in terms of molecular contributions. It is found that the experimentally observed relative insensitivity of the dephasing rate of the fundamental to the thermodynamic condition (between the triple point and the boiling point and above)[9] arises because of an increase in the mean square frequency value $\langle \Delta\omega_{10}^2(0)\rangle$ with a corresponding decrease in the frequency modulation correlation time $\tau_{cn,n=1}$ as the system moves toward the triple point. Another important finding is that the observed sharp rise of the dephasing rate near the critical point is partly due to the *sharp rise in the contribution of the vibration−rotation coupling*. We find that the latter is also responsible, in an unusual way, for the predicted subquadratic quantum number dependence of overtone dephasing in supercritical fluids. Also, our investigations on the temperature−density dependence of the overtone dephasing rate reveal an interesting crossover behavior, pronounced for higher overtones, in the liquid−gas phase transition region for the rates of dephasing. The crossover behavior is weak for the fundamental.

One point of concern, expressed earlier, is the failure of these simulations to provide quantitative agreement with (say, within 10% of) the experimental results; the simulations are off, on the average, by 40%. While this is not fully unexpected, one would still like to explore the possible reason for the discrepancy. There are clearly two main reasons. First, the pair potential might not be system invariant, as assumed in this work. While it may be possible to simulate a vibration directly using ab initio methods, the very high frequency of the N−N vibration (2526 cm^{-1}) makes such a study to be subject to extensive numerical computation and, therefore, possibly statistical errors. Second, as the dephasing is determined by a rather large number of terms, small errors in some of them might lead to a noticeable discrepancy. Both points deserve further studies. Also, high-temperature simulation studies might involve a considerable amount of error and can partly explain the larger discrepancies observed in studies near the critical point and beyond.

It must be stressed here that N_2 was modeled as two neutral Lennard-Jones spheres separated by a bond. In reality, the nitrogen molecule is known to carry a significant quadrupole moment. The quadrupolar interactions among molecules may significantly contribute to the mean square force at the initial time. Relaxation of the quadrupolar contribution to the frequency modulation can be fast and Gaussian at short times. Both these effects will tend to lower the value of the dephasing time.

However, earlier simulation studies of vibrational dephasing in liquid nitrogen using a multiparameter potential which includes short-range valence, dispersion, and quadrupole interactions have reported observable differences of only about 10% or less in the properties of liquid N_2, between the simulations carried out with and without the quadrapolar forces, even near the solid phase.[2b,35] The quadrupolar forces are, therefore, not expected to change the proposed scenario drastically. Electrostatic interactions[50] can also be partly included via the quadrupole−quadrupole interactions but are expected to be quite significant only in dense solid phases. As emphasized earlier, our aim here is to study the possible origin of subquadratic quantum number dependence of vibrational dephasing. Nevertheless, the importance of the quadrupolar interactions on vibrational dephasing of liquid and gaseous nitrogen needs to be investigated.

Also, the use of a multiparameter potential which includes the vibrational−rotational coupling such as the one used by Oxtoby et al.[2b] would have been more appropriate as this would have allowed the accomodation of cross-correlation effects between VR and AA contributions. The observations reported in ref 2b clearly revealed that the combined effect of the cross-correlation effects of the vibration−rotation coupling with the other factors, though relatively small in comparison to cross-correlations between other factors, tends to give rise to a more rapidly relaxing frequency modulation correlation function and, therefore, a longer dephasing time. The estimated dephasing times are found to be less than the experimental reported values at several state points studied in this work. The noninclusion of the cross-correlation effects between the vibration−rotation coupling and the atom−atom contributions, therefore, might partly explain the discrepancies observed between our reported results and experiments.

It should also be pointed out that the simulation system comprises only rigid bond diatomics to obtain the forces on the normal coordinate. As discussed by Berne and co-workers,[34] the time correlation functions of the forces for the rigid bond can be different from those for a real, flexible bond, particularly for medium-high-frequency modes (such as C−I stretching vibration $\simeq$525 cm^{-1} [33]), which could be important for a high overtone state. For N_2, however, such differences may not be significant because of the very high frequency of the N−N vibration. A direct simulation of vibrating molecules is extremely difficult. Nevertheless, one could use the new simulation techniques like RESPA or NAPA[34] to incorporate the effects of the vibrations on the structure and dynamics of the surrounding solvent molecules, though this involves a lot of computational time.

The simulation study considered the frequency modulation as the only mechanism which could lead to deviations from Kubo−Oxtoby theory. For triatomic and other polyatomic molecules, there can be additional dephasing mechanisms such as the off-diagonal anharmonic coupling between different

modes of the polyatomic molecule and the enhanced possibility of resonant energy transfer which[1,3] can contribute to the subquadratic quantum number dependence. Clearly, these mechanisms are absent for nitrogen and also for the cyanide ion[51] and seem unlikely for the C−I stretch of methyl iodide.[6,14] However, these other mechanisms are certainly likely candidates which need to be explored for other systems.

Acknowledgment. We thank Professor J. L. Skinner for helpful conversations. This work was supported in part by grants from the Council of Scientific and Industrial Research, Department of Science and Technology (India), and by the Theoretical Chemistry Institute at the University of Wisconsin at Madison. N.G. thanks CSIR (India) for her Research Fellowship.

References and Notes

(1) Oxtoby, D. W. *J. Chem. Phys.* **1979**, *70*, 2605.
(2) (a) Oxtoby, D. W. *Adv. Chem. Phys.* **1979**, *40*, 1. (b) Oxtoby, D. W. *Annu. Rev. Phys. Chem.* **1981**, *32*, 77; *Adv. Chem. Phys.* **1981**, *47*, 487.
(3) Laubereau, A.; Kaiser, W. *Rev. Mod. Phys.* **1978**, *50*, 607.
(4) Schroeder, J.; Schiemann, V. H.; Sharko, P. T.; Jonas, J. *J. Chem. Phys.* **1977**, *66*, 3215. Doge, G.; Arndt, R.; Khuen, A. *Chem. Phys.* **1977**, *21*, 53.
(5) Laubereau, A.; Kaiser, W. *Annu. Rev. Phys. Chem.* **1975**, *26*, 83.
(6) Myers, A.; Markel, F. *Chem. Phys.* **1990**, *149*, 21.
(7) Schweizer, K. S.; Chandler, D. *J. Chem. Phys.* **1982**, *76*, 2296.
(8) (a) Tominaga, K.; Yoshihara, K. *Phys. Rev. Lett.* **1995**, *74*, 3061. (b) Tominaga, K. In *Advances in Multi-Photon Processes and Spectroscopy*; World Scientific: Singapore, 1998; Vol. 11. (c) Tominaga, K.; Yoshihara, K. *J. Chem. Phys.* **1996**, *104*, 1159. (d) Tominaga, K.; Yoshihara, K. *J. Chem. Phys.* **1996**, *104*, 4419.
(9) Clouter, M. J.; Kiefte, H. *J. Chem. Phys.* **1977**, *66*, 1736.
(10) Clements, W.; Stoicheff, B. P. *Appl. Phys. Lett.* **1968**, *12*, 246.
(11) Scotto, M. *J. Chem. Phys.* **1968**, *49*, 5362.
(12) Brueck, S. R. J. *Chem. Phys. Lett.* **1977**, *50*, 516.
(13) Gayathri, N.; Bagchi, B. *Phys. Rev. Lett.* **1999**, *82*, 4851.
(14) Gayathri, N.; Bhattacharyya, S.; Bagchi, B. *J. Chem. Phys.* **1997**, *107*, 10381.
(15) Le Duff, Y. *J. Chem. Phys.* **1973**, *59*, 1984.
(16) Hesp, H. M. M.; Langelaar, J.; Bebelaar, D.; Van Voorst, J. D. W. *Phys. Rev. Lett.* **1977**, *39*, 1376.
(17) Wright, R. B.; Schwartz, M.; Wang, C. H. *J. Chem. Phys.* **1973**, *58*, 5125.
(18) Jones, D. R.; Anderson, H. C.; Pecora, R. *Chem. Phys.* **1975**, *9*, 339. Patterson, G. D.; Griffiths, J. E. *J. Chem. Phys.* **1975**, *63*, 2406.
(19) Hyde Campbell, J.; Fisher, J. F.; Jonas, J. *J. Chem. Phys.* **1974**, *61*, 346.
(20) Fischer, S. F.; Laubereau, A. *Chem. Phys. Lett.* **1975**, *35*, 6.
(21) Oxtoby, D. W.; Levesque, D.; Weis, J. J. *J. Chem. Phys.* **1978**, *68*, 5528.
(22) Oxtoby, D. W.; Levesque, D.; Weis, J. J. *J. Chem. Phys.* **1980**, *72*, 2744.
(23) Westlund, P. O.; Lynden-Bell, R. *Mol. Phys.* **1987**, *60*, 1189. Lynden-Bell, R.; Westlund, P. O. *Mol. Phys.* **1987**, *61*, 1541. Westlund, P. O.; Lynden-Bell, R. *Chem. Phys. Lett.* **1989**, *154*, 67.
(24) Lynden-Bell, R. *Mol. Phys.* **1977**, *33*, 907.
(25) Vanden Bout, D.; Muller, L. J.; Berg, M. *Phys. Rev. Lett.* **1991**, *67*, 3700.
(26) Muller, L. J.; Vanden Bout, D.; Berg, M. *J. Chem. Phys.* **1993**, *99*, 810.
(27) Inaba, R.; Tominaga, K.; Tasumi, M.; Nelson, K. A.; Yoshihara, K. *J. Chem. Phys.* **1993**, *99*, 810.
(28) Zimdars, D.; Tokmakoff, A.; Chen, S.; Greenfield, S. R.; Fayer, M. D.; Smith, T. I.; Schwettman, H. A. *Phys. Rev. Lett.* **1993**, *70*, 2718.
(29) Kiefer, W.; Bernstein, H. J. *J. Raman Spectrosc.* **1973**, *1*, 417.
(30) Battaglia, M. R.; Madden, P. A. *Mol. Phys.* **1978**, *36*, 1601.
(31) Sjogren, L.; Sjolander, A. *J. Phys. Chem.* **1979**, *12*, 4369.
(32) Bhattacharya, S.; Bagchi, B. *J. Chem. Phys.* **1997**, *106*, 1757. Bhattacharyya, S.; Bagchi, B. *J. Chem. Phys.* **1997**, *106*, 7262.
(33) Gayathri, N.; Bagchi, B. *J. Chem. Phys.* **1999**, *110*, 539.
(34) Berne, B. J.; Tuckerman, M. E.; Straub, J. E.; Bug, A. L. R. *J. Chem. Phys.* **1990**, *93*, 5084. Tuckerman, M.; Berne, B. J.; Martyna, G. J. *J. Chem. Phys.* **1992**, *97*, 1990. Tuckerman, M.; Berne, B. J. *J. Chem. Phys.* **1993**, *98*, 7301.
(35) Cheung, P. S. Y.; Powles, J. G. *Mol. Phys.* **1975**, *30*, 921.
(36) Wertheimer, R. *Mol. Phys.* **1978**, *35*, 257.
(37) Amotz, D. B.; Herschbach, D. *J. Phys. Chem.* **1990**, *94*, 1038.
(38) Khan, I. A.; Ayappa, K. G. *J. Chem. Phys.* **1998**, *109*, 4576.
(39) Crawford, R. K.; Daniels, W. B.; Cheng, V. M. *Phys. Rev. A* **1975**, *12*, 1690.
(40) Balucani, U.; Zoppi, M. *Dynamics of the Liquid State*; Clarendon Press: Oxford, 1994; and references therein.
(41) Ravichandran, S.; Bagchi, B. *J. Phys. Chem.* **1994**, *98*, 11242; *Int. Rev. Phys. Chem.* **1995**, *14*, 271.
(42) Berne, B. J.; Harp, G. D. *Adv. Chem. Phys.* **1970**, *17*, 63.
(43) Frankland, S. J. V.; Maroncelli, M. Preprint.
(44) Powles, J. G.; Murad, S.; Sethi, D. P.; Ravi, P. V. *Mol. Phys.* **1991**, *73*, 1307.
(45) Chesnoy, J. *Chem. Phys. Lett.* **1986**, *125*, 267.
(46) Musso, M.; Asenbaum, A.; Deutel, D.; Seifert, F.; Oehme, K.-L. *Phys. Rev. Lett.* **1996**, *77*, 2746.
(47) Mukamel, S.; Stern, P. S.; Ronis, D. *Phys. Rev. Lett.* **1983**, *50*, 590.
(48) Adams, J. E. *J. Phys. Chem. B* **1998**, *102*, 7455.
(49) Tucker, S.; Maddox, M. W. *J. Phys. Chem. B* **1998**, *102*, 2437.
(50) Cardini, G.; Oshea, S. F.; McDonald, I. R. *Mol. Phys.* **1991**, *73*, 1307.
(51) Hamm, P.; Lim, M.; Hochstrasser, R. M. *J. Chem. Phys.* **1997**, *107*, 10523.